# DEVELOPMENT OF DAMAGE FUNCTION FOR SEISMIC RISK ASSESSMENT FOR SEMI-CONDUCTOR MANUFACTURING PLANT

**Itsuki KAWAKUBO**
*InterRisk Research Institute & Consulting, Inc., Japan*

**Kei HORIE**
*InterRisk Research Institute & Consulting, Inc., Japan*

**SUMMARY:**
The purpose of this research was to develop a damage function for a semiconductor manufacturing plant that includes building, content, and business interruptions. First of all, typical seismic damages for semiconductor (semi-con) plant from the Great Tohoku Earthquake in 2011 were summarized. Then, to estimate building damage, capacity curve was developed for some actual semi-con plant building. Damage functions for semi-con manufacturing devices was also formulated using event tree model. Finally damage functions for business interruptions were developed based on perfect correlation condition while many phenomena on a manufacturing plant which subjected to earthquake event are affected each others. As a result, we found a semi-con plant is more vulnerable than general industrial plant at the low seismic load level.

*Keywords: Risk Assessment, Damage Function, Vulnerability Function, Semiconductor manufacturing plant*

## 1. INTRODUCTION

The semiconductor (semi-con) industry reported tremendous damage caused by the Great Tohoku earthquake. However, most of the damage was to the content; severe building damage was not observed in this earthquake. Thus, manufacturing device and nonstructural seismic resistance design should be considered more seriously, while building design performed effectively. The main devices for semi-con manufacturing, such as the optical aligner, generally cost no less than ¥10 billion per device and are easily damaged by nonstructural failures such as ceiling or grating panels falling down. To keep the indoor air clean, the manufacturing area is designed to clean room specifications; this means that the manufacturing area is sandwiched by ceiling/floor panels accompanying a dense duct network. We developed a damage function that comprehensively covers the building, content, and business interruption (BI) of a semi-con plant. The typical damage features of a semi-con plant are introduced in section 2. The building, content, and BI damage estimation methods are described in the following sections.

## 2. DAMAGE SUMMARY FROM THE 2011 GREAT TOHOKU EARTHQUAKE

Several earthquake-damaged semi-con manufacturing plants reported that their operation was affected by device damage rather than building damage. Two typical damage causes can be derived from these reports. One is a malfunction of the devices themselves. Semi-con manufacturing devices require a high level of precision to their settings and are very sensitive to setting errors. Once they are displaced even slightly, they have to be rearranged very carefully. The other is nonstructural damage to building components such as the ceiling, wall boards, grating panels, ceiling ducts, and cable racks. When these parts are damaged and fall onto the devices, they cause damage that can be very costly (see Table 2.1). The story level was also reported to affect the severity level of damage: i.e., devices located on higher stories tended to be more severely damaged due to acceleration amplification relative to the ground floor level. In other words, device resistance design can be weighted according to the story level.

**Table 2.1.** Damage summary for devices and nonstructural components

| Damage type | Damaged parts | Damage situation |
|---|---|---|
| Device damage | Device body | Displacement, overturning, falling to floor, liquid spill |
| | Attachment | Deformation, breakage |
| | Half-finished parts | Falling down, collision, displacement |
| | Vacuum pumping | Breakage |
| Non-structural damage | Ceiling duct/cable/panel | Water leakage, falling down |
| | Wall board/partition | Deformation, falling down, crack |
| | Floor/grating panel | Liquid spill, disjoint, caving |

## 3. EVALUATION BUILDING CAPACITY SPECTRA

This section presents the evaluation of a capacity curve for a semi-con manufacturing building. The capacity curves modeled here are used to estimate the maximum displacement by the capacity spectra method in the next step.

### 3.1. Modeled buildings

Three average manufacturing buildings are discussed here to consider the maximum displacement response when subjected to an earthquake load. Their structural profiles were based on actual structural calculation reports. Two were low-rise buildings (1–3 stories), and the third was a middle-rise building (4–6 stories). Six structural models in all were set by considering two analysis directions for each building. The structure type was steel moment frames with braces. None of the buildings were equipped with special seismic resistance systems such as base isolation or dampers. The structural building profiles are outlined in Table 3.1.

**Table 3.1.** Structural building profiles

| Type of building | Average story height [m] | Average floor mass [kN] | Average initial stiffness [kN/cm] |
|---|---|---|---|
| Low-rise (1–3 stories) | 6.2 | 53,122 | 32,366 |
| Mid-rise(4–6 stories) | 7.1 | 229,911 | 95,694 |

### 3.2. Evaluating building capacity spectra

The abovementioned models were used for pushover analysis. The lateral force distribution was defined according to the Japanese building design code, i.e., *Ai* distribution. The *Ai* distribution is calculated using the natural period, which is simply derived from the building height and each story's mass for the seismic load. The lateral force is loaded statically until its maximum displacement reaches 1/25. The $S_a$–$S_d$ relation of each model was evaluated using the following equations.

$$S_a = \frac{Q}{M} \tag{3.1}$$

$$M = \frac{\left(\sum m_i \cdot \delta_i\right)^2}{\sum m_i \cdot \delta_i^2} \tag{3.2}$$

$$S_d = \frac{\sum m_i \cdot \delta_i^2}{\sum m_i \cdot \delta_i} \tag{3.3}$$

where $Q$ is the base shear force, $M$ is the effective mass, $m_i$ is the mass of story $i$, and $\delta_i$ is the displacement of story $i$. After the pushover analysis, the $S_a$–$S_d$ relation was modeled into a trilinear curve from an energy equivalence point of view. Each $S_a$–$S_d$ trilinear curve was averaged into a single curve. After the maximum response displacement is calculated for an individual response spectrum, the building damage loss is estimated. Each story drift ratio is calculated from $S_d$, and corresponding repair costs are accumulated to a total loss of the building.

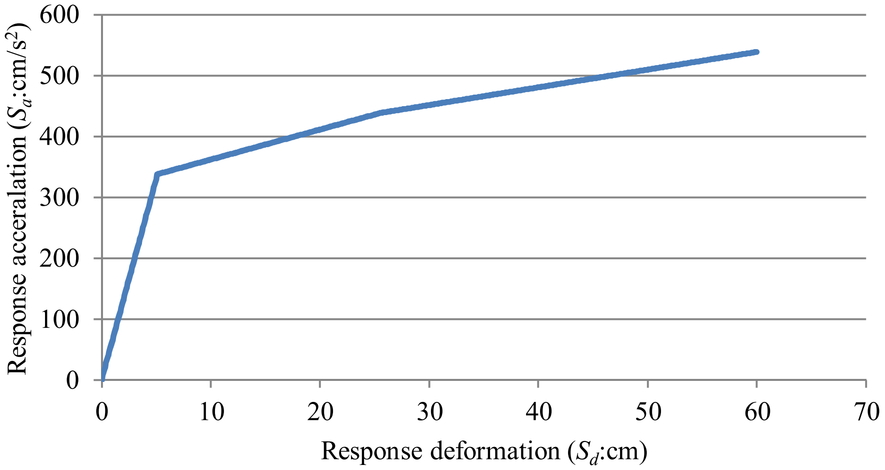

(a) Low-rise building

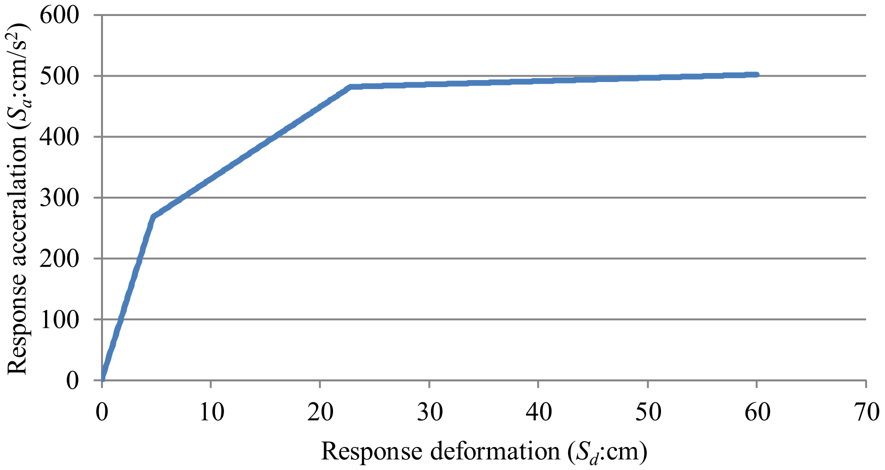

(b) Mid-rise building

**Figure 3.1.** Average capacity curve

## 4. CONTENT DAMAGE ESTIMATION

In this paper, "content" refers to equipment for semi-con manufacturing, such as optical aligners and ion implanters. In general, such equipment is very expensive and takes a long time to replace. First, an event tree model was introduced to consider all type of seismic damage to these equipment. We then applied median capacity values in terms of floor response acceleration to each potential damage mode of the equipment. These median capacity values were derived from actual surveys or an analytical approach. Finally, we combined these equipment fragility curves into a single floor representative damage function according to replacement value weighting.

### 4.1. Damage ratio derivation

The damage function for each equipment is described below.

$$D_R(\alpha)=\sum_{i=1}^{n}P_i(\alpha)\cdot C_i \tag{2.1}$$

$P_i(\alpha)$ denotes the type $i$ damage mode occurrence probability owing to maximum floor acceleration α for the story the equipment is located on. $C_i$ denotes the damage ratio corresponding to the type $i$ damage mode. $n$ denotes the number of damage mode types.

The damage function derivation procedure is described graphically below. This example is a case where the occurrence probabilities for moderate and severe damage are 0.30 and 0.10, respectively, and the corresponding damage ratios are 0.2 and 1.0, respectively.

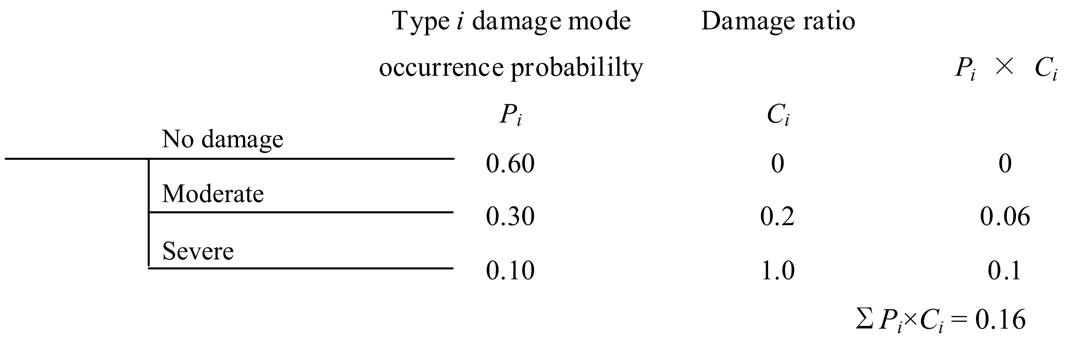

| | Type $i$ damage mode occurrence probabililty $P_i$ | Damage ratio $C_i$ | $P_i \times C_i$ |
|---|---|---|---|
| No damage | 0.60 | 0 | 0 |
| Moderate | 0.30 | 0.2 | 0.06 |
| Severe | 0.10 | 1.0 | 0.1 |
| | | | $\Sigma P_i \times C_i = 0.16$ |

**Figure 4.1.** Accumulation of damage ratio

## 4.2. Event tree model

The evaluation of the damage function is described in detail here using the event tree model. Fig. 4.2 shows a simple procedure for incorporating certain multiple damage modes. There are three damage modes in this example: type 1 causes 100% loss, type 2 causes 30% loss, and type 3 causes 10% loss. The damage mode types 1–3 occur compositely when the structure is subjected to a seismic load. Fig. 4.2 shows all possible routes to five different damage ratios. The arrows in the figure show the possible routes: i.e., damage type 1 is not observed when damage types 2 and 3 occur. The damage ratio is then calculated as 40% by adding 30% from type 2 and 10% from type 3. Note that 100% loss occurs once damage mode type 1 is observed. Five semi-con manufacturing device event trees were developed in this study; however, only two are shown in the following section owing to space limitations.

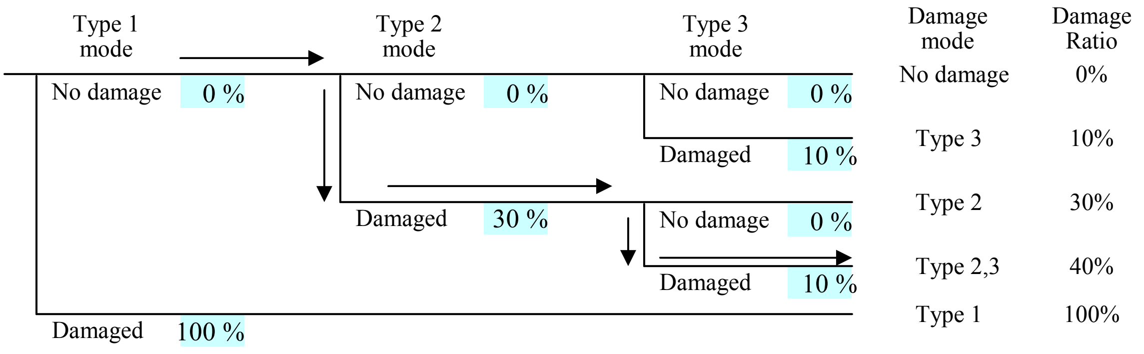

**Figure 4.2.** Basic concept for event tree model

### *4.2.1. Optical aligners*

Fig 4.3. shows the event tree for optical aligners, which include a sequential process for patterning wafers. Five damage modes of the optical aligner are as follows: damage to the entire device body, light axis shift, wafer stage shift, lens damage, conveyance robot damage, and wafer stage/reticle stage damage. In addition to the above damage modes, major damage to the entire body includes all other damage modes. Major damage to the entire body results in a damage ratio of 100%. Thus, there are 65 (= $2^6 + 1$) possible damage routes. Each damage ratio shown here was derived from a survey of historical seismic damage to semi-con plants.

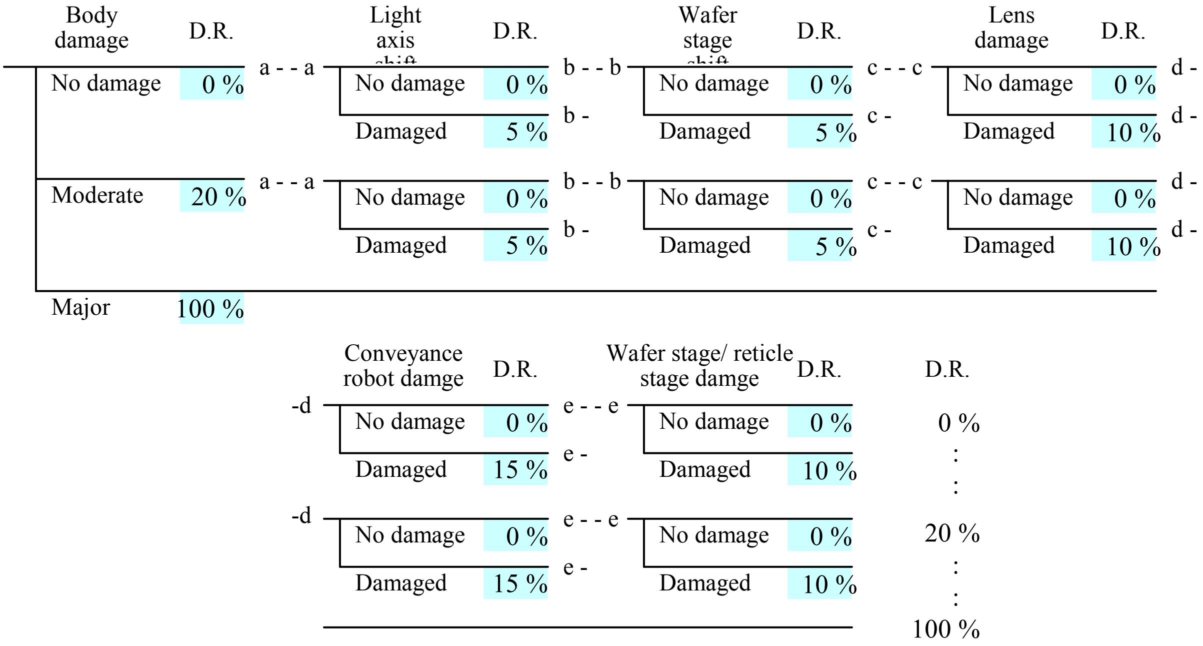

**Figure 4.3.** Event tree for optical aligners

*4.2.2. Ion implanter*

The event tree for ion implanters is presented here. The ion implanter includes a process for implanting ion dopants into a solid in an electrical field. There are three damage modes for an ion implanter: body damage, beam/scanning system damage, and high voltage tank damage. Grating panel damage is also considered if the device is on a grating panel (see Fig. 4.4). We assumed that 10% of the ion implanters are located on gratings. Thus, there are 19 (= $2 \times 3^2 + 1$) or 37 (=$2 \times 3^2 \times 2 + 1$) possible damage routes depending on whether grating damage is considered.

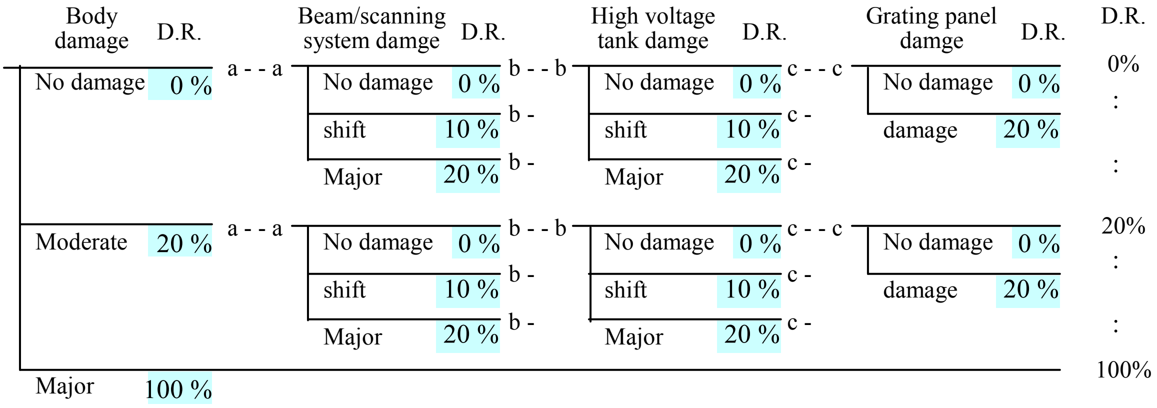

**Figure 4.4.** Event tree for ion implanters

## 4.3. Device fragility information

Table 4.1 shows the median capacity values of each manufacturing device. The median capacity is described by the maximum floor acceleration, and according to its definition, the probability that a certain damage mode occur is 50% at median capacity. For example, the optical aligner main body has a 50% probability to sustain moderate damage at 790 cm/s$^2$ and major damage at 1590 cm/s$^2$.

**Table 4.1.** Median capacity for each damage mode

| Equipment | Damage type | Damage state | Median capacity (cm/s$^2$) | |
|---|---|---|---|---|
| | | | On floor slab | On grating |
| Optical aligners | Main body damage | Moderate | 790 | - |
| | | Major | 1590 | - |
| | Light axis shift | Occurred | 200 | - |
| | Wafer stage shift | Occurred | 200 | - |
| | Lens damage | Occurred | 330 | - |
| | Conveyance robot damage | Occurred | 520 | - |
| | Wafer stage/Reticle stage damage | Occurred | 520 | - |
| Ion implanter | Main body damage | Moderate | 780 | 1000 |
| | | Major | 1560 | 2000 |
| | Beam/scanning system damage | Shift | 390 | 300 |
| | | Major | 520 | 400 |
| | High voltage tank damage | Shift | 390 | 300 |
| | | Major | 520 | 400 |
| | Grating panel damage | Major | - | 900 |
| CVD device<br>CVD:Chemical Vapor Deposition | Main body damage | Moderate | 820 | 950 |
| | | Major | 1650 | 1890 |
| | Quartz tube damage | Occurred | 100 | 80 |
| | Ceramic parts damage | Occurred | 100 | 80 |
| | Conveyance robot damage | Occurred | 520 | 400 |
| | Control system error | Occurred | 520 | 400 |
| | Shower head/heater/lamp damage | Occurred | 780 | 600 |
| | Grating panel damage | Major | - | 900 |
| Wet etching device | Main body damage | Moderate | 850 | 1000 |
| | | Major | 1690 | 2010 |
| | Grating panel damage | Major | - | 900 |
| CMP device<br>CMP:Chemical-Mechanical Planarization | Main body damage | Moderate | 820 | 930 |
| | | Major | 1640 | 1860 |
| | Axis shift | Occurred | 520 | 400 |
| | Conveyance error | Occurred | 650 | 500 |
| | Pipe and drain damage | Occurred | 650 | 500 |
| | Grating panel damage | Major | - | 900 |

The vertical axis of the fragility curve shows the probability for the occurrence of a certain damage mode, and the horizontal axis is the maximum floor acceleration. The fragility curve is approximated by integrating the log-normal distribution using the median capacity for average. A log-normal standard deviation of 0.3 was assumed here. The uncertainty of the ground motion was also considered as 0.6 of the standard deviation; thus, the obtained composite standard deviation was 0.67 based on the square-root of the sum of the squares of 0.6 and 0.3. The composite standard deviation was regarded as an accumulation of the capacity and ground motion variability blending. The median capacity values corresponding to each damage type and mode were derived from onsite surveys.

The fragility curve for the device body damage and light axis shift of optical aligners were plotted (see Fig. 4.5.) The figure indicates a 25% probability of major damage, 40% probability of moderate damage (= 65% − 25%), and 35% probability of no damage (= 100% − 65%) to the body at floor acceleration of 1000 cm/s$^2$. The light axis shift has 50% and 85% chances of being damaged at accelerations of 200 and 400 cm/s$^2$, respectively. It should be noted that damage to the light axis shift occurs at low floor acceleration levels. Similarly, damage to the wafer stage shift and to the quartz tube and ceramic parts of the CVD device, which have small median capacity, is also likely to occur at a low floor acceleration. The vertical axis of the damage function indicates a ratio derived by dividing the loss amount by its replacement value, and the horizontal axis indicates the floor response acceleration. Note that only content damage caused by shaking was considered in this study; content damage due to clean room disability or utility shut down was not considered.

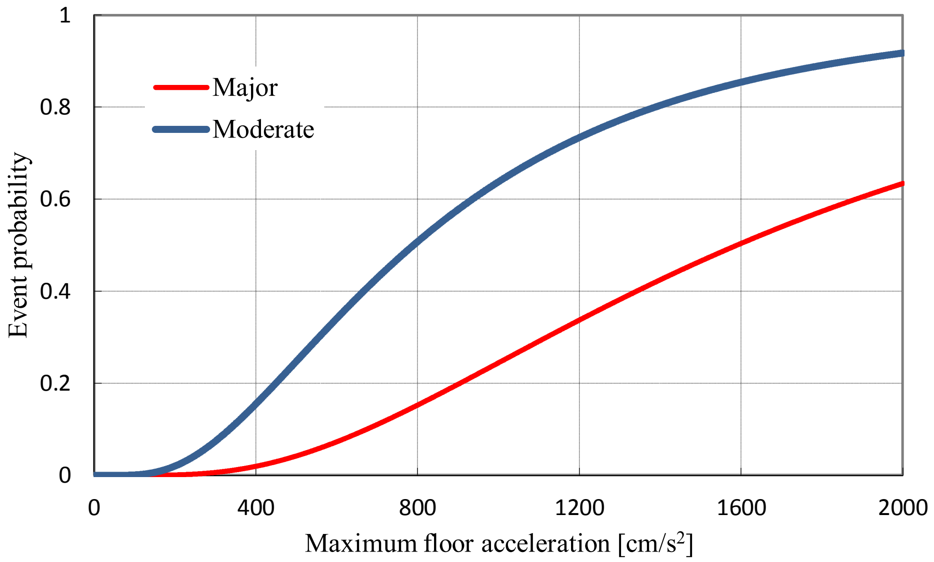

(a) Optical aligner device body

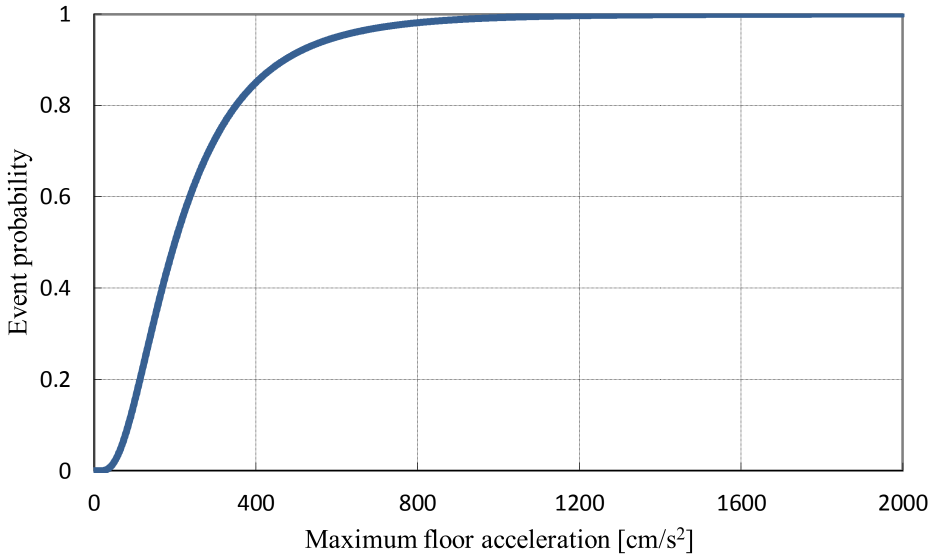

(b) Light axis shift

**Figure 4.5.** Fragility curve for optical aligners

## 4.4. Device replacement values

In order to represent the floor fragility for five devices, the replacement value weighted average was introduced. In general, a single manufacturing floor generally has 3–10 optical aligners, ion implanters, wet etching devices, and CMP devices and 30–40 CVD devices. We used the maximum number of each device and average replacement value (see Table 4.2).

**Table 4.2.** Fraction of device replacement value per floor

| | Optical aligners | Ion implanter | CVD | Wet etching | CMP | Floor all |
|---|---|---|---|---|---|---|
| Replacement value[Mil. Yen/unit] | 500 | 250 | 25 | 15 | 30 | - |
| Number of unit on 1 floor | 10 | 10 | 50 | 10 | 10 | - |
| Replacement value[Mil. Yen/floor] | 5000 | 2500 | 1250 | 150 | 300 | 9200 |
| Fraction of replacement value | 54% | 27% | 14% | 2% | 3% | 100% |

## 4.5. Floor representative damage function

The floor representative damage function was evaluated according to the replacement value weight, as shown in Table 4.2 (see Fig. 4.6.). These damage functions were modeled using a composite standard deviation value of 0.67. We assumed that a maximum of half the devices would have major damage. Thus, each damage function curve approaches 0.5 asymptotically. If the floor is subjected to an acceleration of 300 cm/s$^2$, the representative floor damage ratio will be 0.1; similarly, a floor acceleration of 600 cm/s$^2$ causes a damage ratio of 0.2.

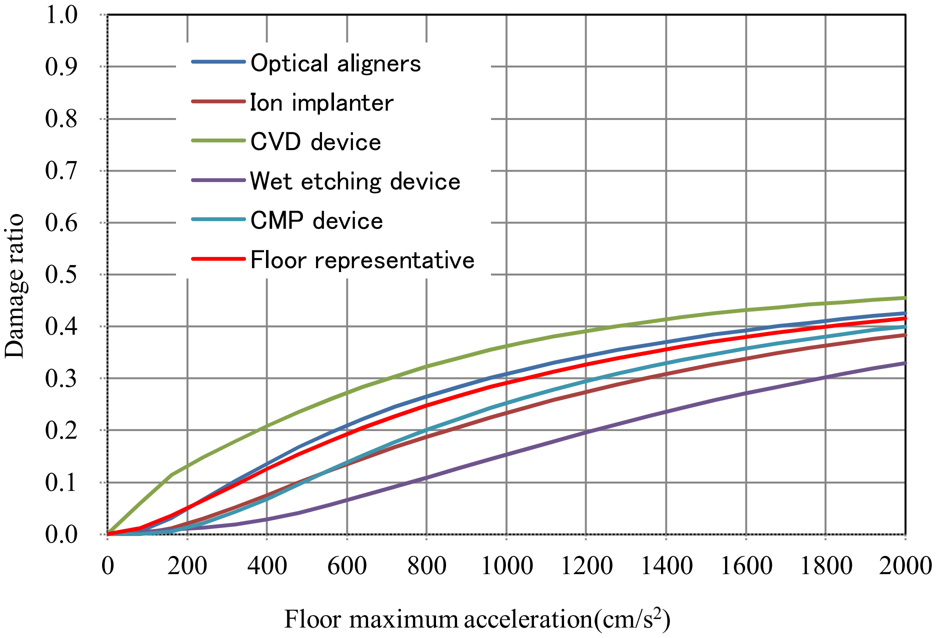

**Figure 4.6.** Results of floor damage function evaluation

## 5. BUSINESS INTERRUPTION

In this paper, business interruption is defined by how long it takes for the manufacturing devices to recover from the seismic damage. Note that it does not consider recovery from utility damage or a breakdown in the supply chain.

### 5.1. Evaluation of recovery system with perfect correlation

Many semi-con manufacturing systems consist of a variety of manufacturing devices connected in parallel or tandem to each other (see Fig. 5.1); processes connected in parallel have similar vulnerabilities. If the correlation among phenomena is assumed to be perfect, the manufacturing system is re-described as a tandem line (see Fig. 5.2). Nakamura et al[3]. proposed that correlation between two devices can be estimated using variances of damage probability distribution and seismic load probability distribution as the following equations:

$$\rho_{F12} = \frac{\mathrm{var}(\ln X)}{\sqrt{\mathrm{var}(\ln F_1)} \cdot \sqrt{\mathrm{var}(\ln F_2)}} \tag{5.1}$$

where $\rho_{F12}$ is correlation of device 1, and 2 damage phenomena, $F_1$, $F_2$ are damage probabilities which caused by a seismic load $X$. Furthermore, this equation is re-described using logarithm standard deviation $\zeta_X$, $\zeta_{F1}$, and $\zeta_{F2}$,

$$\rho_{F12} = \frac{\zeta_X^{\,2}}{\zeta_{F1}\zeta_{F2}} \tag{5.2}$$

$\zeta_{F1}$ and $\zeta_{F2}$ are composite deviation with seismic load's standard deviation, and described as follows:

$$\zeta_{Fi} = \sqrt{\zeta_{Ci}^{\,2} + \zeta_X^{\,2}}, \quad i = 1, 2 \tag{5.3}$$

where $\zeta_{C1}$, $\zeta_{C2}$ are logarithm standard deviation of devices' resistance capacity against seismic load. The uncertainty of seismic load is considered 0.5 − 0.7 in logarithm standard deviation and the uncertainty of resistance capacity is 0.2 at most. Thus, the correlation of damage is estimated as 0.86 − 0.92 from Eqn. 5.2. and Eqn. 5.3. Similar equipments are presumed to have higher correlations. Finally, we can assume perfect correlation on to semi-con manufacturing business interruptions.

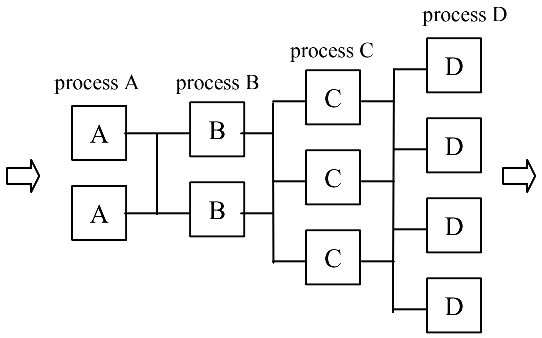

**Figure 5.1.** General manufacturing system

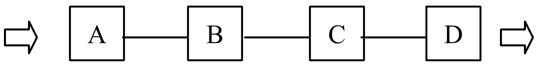

**Figure 5.2.** System assuming perfect correlation

## 5.2. Application to semi-con manufacturing devices

The recovery time for semi-con manufacturing devices was evaluated using the method discussed in the previous section. Table 5.1 lists the median capacity and corresponding recovery time for each damage type. We assumed that these devices were all located on one floor.

**Table 5.1.** Capacity median and recovery time

| Equipment | Damage type | Capacity median ($cm/s^2$) | Recovery time (days) |
|---|---|---|---|
| Optical aligners | Quartz tube damage | 100 | 7 |
| | Main body damage moderate | 790 | 14 |
| | Main body damage major | 1590 | 180 |
| Ion implanter | Beam/Scanning system damage | 390 | 7 |
| | Main body damage moderate | 780 | 14 |
| | Main body damage major | 1560 | 180 |
| CVD | Quartz tube damage | 100 | 7 |
| | Main body damage moderate | 820 | 14 |
| | Main body damage major | 1650 | 180 |
| Wet etching | Main body damage moderate | 850 | 14 |
| | Main body damage major | 1690 | 180 |
| CMP | Axis shift | 100 | 7 |
| | Main body damage moderate | 820 | 14 |
| | Main body damage major | 1640 | 180 |

Fig. 5.3. shows that relationship between maximum floor acceleration and recovery days. The vertical axis of the damage function represents the recovery days, and the horizontal axis represents the maximum floor acceleration. In the 2004 Chuetsu Earthquake in Niigata prefecture in Japan, a major semi-con manufacturing plant was severely damaged and business interruption lasted eight months to

full recovery of regular production. On the other hand, it took six months for a major plant affected by the 2011 Great Tohoku Earthquake to recover. Both plants were considered to be the worst cases among the damaged plants. Restarting semi-con production needs a certification process to ensure quality and reliability after the practical recovery of the product line. This generally takes two or three months. Thus, the practical business interruption of the above two cases were recalculated as five and three months, respectively.

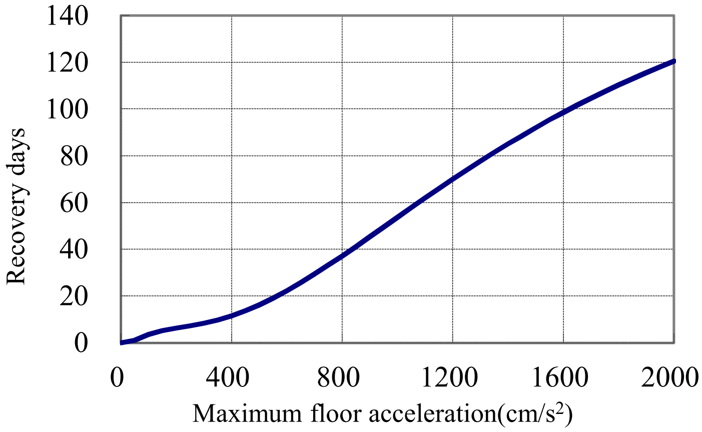

**Figure 5.3.** Expected value of recovery time

## 6. CONCLUSION

We developed a damage function for a semi-con manufacturing plant. According to our idealized analysis for semi-con and general industry plants, the former is more vulnerable than the latter to seismic damage especially at low seismic load level. It has to be tested against a larger number of actual seismic events to confirm the validity of our assumptions. Comprehensive damage estimation for the precision instruments such semi-con industry is important considering the major impact on all over the industry. This study will be the base for future developing vulnerabilities for semi-con industry.

## ACKNOWLEDGEMENT

Dr. Komei Nakamura and Mr. Toshiro Shizuma of the Shinozuka Research Institute made enormous contributions to this paper. Our deepest appreciation goes to them.

## REFERENCES

1) Shibata, A. (2003), New Seismic Design Analysis, Morikita Publishing (in Japanese)
2) Hoshi, M., Nakamura, K. (2002), Seismic Risk Management of Structure, Sankaido Publishing (in Japanese)
3) Nakamura, K et al.(2011), A Study of System Performance Evaluation Due to Eearthquake with Damage Correlation. *Journal of Structural And Construction Engineering* **Vol.76** No.661, 713-719 (in Japanese)
4) Kawakubo, I., Horie, K. (2011). Development of damage function for seismic risk assessment for equipments of Semiconductor manufacturing plant. *Proceedings* for *AIJ Annual Conference (Kanto)* **Vol. 4**, p. 918 (in Japanese)